MgATP-Dependent Activation by Phosphoenolpyruvate of the E187A Mutant of *Escherichia coli* Phosphofructokinase†

Audrey S. Pham*,‡ and Gregory D. Reinhart§

Division of Pathology and Laboratory Medicine, The University of Texas M. D. Anderson Cancer Center, Houston, Texas 77030, and Department of Biochemistry and Biophysics, Texas A&M University, College Station, Texas 77843

Received July 28, 2000; Revised Manuscript Received October 30, 2000

ABSTRACT: Using enzymatic assays and steady-state fluorescence emission, we performed a linkage analysis of the three-ligand interaction of fructose 6-phosphate (Fru-6-P), phosphoenolpyruvate (PEP), and MgATP on E187A mutant *Escherichia coli* phosphofructokinase (PFK). PEP allosterically inhibits Fru-6-P binding to *E. coli* PFK. The magnitude of antagonism is 90-fold in the absence and 60-fold in the presence of a saturating concentration of MgATP [Johnson, J. J., and Reinhart, G. D. (1997) *Biochemistry 36*, 12814−12822]. Substituting an alanine for the glutamate at position 187, located in the allosteric site (i.e., mutant E187A), activates Fru-6-P binding and inhibits the maximal rate of enzyme turnover [Lau, F. T.-K., and Fersht, A. R. (1987) *Nature 326*, 811−812]. The allosteric action of PEP appears to depend on the presence of the cosubstrate MgATP. In the presence of a saturating concentration of MgATP, PEP enhances the binding of Fru-6-P to the enzyme by a modest 2-fold. Decreasing the concentration of MgATP mitigates the extent of activation. At MgATP concentrations approaching 25 μM, PEP becomes insensitive to the binding of Fru-6-P. At MgATP concentrations <25 μM, PEP "crosses over" and becomes antagonistic toward substrate binding. The present study examines the role of Glu 187 at the allosteric site in the binding of Fru-6-P and offers a more complex explanation of the mechanism than that described by traditional allosteric mechanistic models.

Phosphofructokinase (PFK)[1] from *Escherichia coli* catalyzes a γ-phosphoryl transfer reaction from MgATP and fructose 6-phosphate (Fru-6-P) to form fructose 1,6-bisphosphate and MgADP. Phosphoenolpyruvate (PEP) is a PFK allosteric inhibitor that binds to a remote site and decreases the binding affinity of Fru-6-P to the enzyme. In the wild-type *E. coli* PFK, PEP alters only the apparent binding affinity of Fru-6-P (*K*-type) and not the maximal rate of enzyme turnover (*V*-type). Workers have proposed that the allosteric response of PEP is mediated predominately by Glu 187 (*1*−*3*). Crystallographic data suggest that the carboxyl of Glu 187 actively participates in the binding of both the activator and the inhibitor (*4*−*6*). We previously demonstrated that substituting an alanine for the glutamate at position 187 (i.e., E187A mutant) causes MgADP to lose its allosteric effectiveness, whereas binding remains comparable to that in the wild-type enzyme (*7*). Lau and Fersht reported that mutation of Glu 187 causes PEP to activate rather than inhibit Fru-6-P binding (*1*). Furthermore, the mutation also activates the *V*-type effect, causing a decrease in the efficiency of catalytic turnover (*1*). These actions of PEP in the mutant enzyme were reported in experiments using a saturating concentration of the cosubstrate MgATP (*1*). However, the role of MgATP in Fru-6-P/PEP interactions has not been quantified in past experiments and is thus the focus of the present report.

In the wild-type PFK, the coupling between PEP and Fru-6-P is approximately 90-fold inhibitory ($Q_{ay/b} = 0.011$), yielding a +2.4 kcal/mol coupling free energy and a predominantly enthalpic reaction (*8*). Because the Fru-6-P/PEP coupling is activating in the E187A mutant, we are interested in determining the governing thermodynamic force between PEP and Fru-6-P. Specifically, we want to determine whether the enthalpic reaction (ΔH) changes from positive to negative or whether ΔH and $T\Delta S$ cancel each other, resulting in a "switch" from an enthalpic to an entropic driving force. Furthermore, quantification of the extent of the contribution by MgATP in Fru-6-P/PEP coupling may allow a qualitative assessment of the protein structure's plasticity. In the wild-type enzyme, MgATP only minimally affects the binding of PEP under standard conditions (*8*). The activating and inhibitory effects of MgATP and PEP are only apparent at extreme temperatures. MgATP promotes PEP binding at temperatures <35 °C and antagonizes PEP binding at temperatures ≥35 °C (*8*). In contrast, MgATP exerted a considerable inhibitory effect toward the binding of Fru-6-P, leading to a 60-fold reduction in the affinity of the enzyme for Fru-6-P (*9*). The contribution of MgATP to the Fru-6-P/PEP interaction is a minor, but significant, effect.

† This work was performed (by A.S.P.) at Texas A&M University in partial fulfillment of the dissertation for the Ph.D. in Biochemistry and was supported by Grant GM33216 (to G.D.R.) from the National Institutes of Health.

* To whom correspondence should be addressed at the Division of Pathology and Laboratory Medicine, The University of Texas M. D. Anderson Cancer Center, 1515 Holcombe Blvd., Houston, TX 77030. Phone: 713-792-0729. Fax: 713-792-0936. E-mail: aspham@mail.mdanderson.org.

‡ The University of Texas M. D. Anderson Cancer Center.

§ Texas A&M University.

[1] Abbreviations: The abbreviations and notations are described in the preceding paper (*7*).

10.1021/bi001769r CCC: $20.00
Published on Web 03/07/2001

MgATP acts mainly to mitigate some measure of inhibition between PEP and Fru-6-P (*8*). This alleviation of inhibition can account for the small degree of activation of the coupling between PEP and MgATP when Fru-6-P is present in a saturating concentration, yielding a $Q_{by/a}$ of approximately 1.9 at 25 °C (*8*).

In the wild-type PFK, Fru-6-P is able to achieve a binding equilibrium at steady state (*10*). Thus, the dissociation constant (K_{iF}) for Fru-6-P determined using equilibrium measurements is comparable to that obtained using steady-state kinetics. The Fru-6-P/PEP coupling interactions are routinely quantified by enzymatic assays and require the presence of MgATP. Quantification of the Fru-6-P/PEP interaction in the absence of MgATP is typically performed by monitoring the intrinsic fluorescence emission intensity. The single tryptophan (Trp 311) per homologous subunit of *E. coli* PFK has been extensively utilized as a fluorescent probe to examine ligand binding (*7*−*9*, *11*, *12*). It has been shown that the equilibrium parameters quantified using enzymatic assays are directly comparable to those using fluorescence emission (*10*). Enzymatic assays performed in the presence of a saturating amount of MgATP yield a dissociation constant for Fru-6-P of approximately 0.5 mM. Decreasing MgATP concentrations lead to progressively lower K_d values, resulting in a final extrapolated K_d of 8 μM at zero concentration MgATP. This value is consistent with the dissociation constant obtained from fluorescence emission (*8*).

The coupling constants *Q* and *W* are linkage parameters that describe the ratios of independent (i.e., in the absence of all other ligands) to conditional (i.e., in the presence of a saturating concentration of a second ligand) ligand binding to the enzyme. *Q* describes the magnitude and nature of the *K*-type effect, to which the extent of substrate concentration producing a half-maximal rate is altered by the presence of one or more other ligands. *W* describes the *V*-type effect, to which the maximal rate of activity for one ligand is altered by one or more other ligands. For *Q* and *W*, a value >1 indicates activation, a value <1 indicates inhibition, and a value $= 1$ indicates no allosteric effects. *Q* is related to the Gibbs free energy equation, which can reveal underlying thermodynamic characteristics of a particular linked interaction.

The influence of PEP on the binding of Fru-6-P to PFK in the absence and the presence of MgATP is examined. The respective couplings are represented by the following disproportionation reactions:

$$\text{PEP—PFK} + \text{PFK—Fru-6-P} \overset{Q_{ay}}{\rightleftharpoons} \text{PEP—PFK—Fru-6-P} + \text{PFK}$$

$$\begin{array}{ccccc} \text{PEP—PFK} & + & \text{PFK—Fru-6-P} & \overset{Q_{ay/b}}{\rightleftharpoons} & \text{PEP—PFK—Fru-6-P} \quad + \quad \text{PFK} \\ | & & | & & | \qquad\qquad\quad | \\ \text{MgATP} & & \text{MgATP} & & \text{MgATP} \qquad\quad \text{MgATP} \end{array}$$

$$\begin{array}{ccc} \text{E} + \text{A} & \overset{\Delta G^\circ_a}{\rightleftharpoons} & \text{EA} \\ + & & + \\ \text{X} & & \text{X} \\ \Big\updownarrow \Delta G^\circ_x & & \Big\updownarrow \Delta G^\circ_{x/a} \\ \text{XE} + \text{A} & \overset{\Delta G^\circ_{a/x}}{\rightleftharpoons} & \text{XEA} \end{array}$$

where, conventionally, a = Fru-6-P, b = MgATP, and y = PEP. After determining Q_{ay} and $Q_{ay/b}$ in the absence versus the presence of MgATP, respectively, and after determining Q_{ab} by varying the MgATP concentration, other coupling parameters, such as Q_{by}, $Q_{by/a}$, $Q_{ab/y}$, and Q_{aby}, can be deduced using the identity principle (*8*, *9*, *13*, *14*).

MATERIALS AND METHODS

Materials. All reagents used in buffers, PFK purification, enzyme kinetics, and fluorescence studies, including Fru-6-P (disodium salt), ADP (potassium salt), ATP (disodium salt), and PEP (trisodium salt), were of analytical grade and were purchased from either Sigma Chemical Co. (St. Louis, MO) or Fisher Scientific (Pittsburgh, PA).

Site-Directed Mutagenesis and Expression of the pfk-1 Enzyme. Mutation of the *pfk* gene and expression of the E187A mutant PFK protein have been extensively described (*7*).

Purification of PFK. The PFK purification protocol was performed as described previously (*7*).

Steady-State Kinetics. Kinetic assays were performed as described previously (*7*), with several modifications. Most assays were performed using a 50 mM EPPS−KOH (pH 8) solution containing 100 mM KCl, 10 mM $MgCl_2$, 2 mM dithiothreitol, 0.1 mM EDTA, and 0.2 mM NADH. The variation of an apparent K_a ($K_{1/2}$ for Fru-6-P) was determined as a function of several fixed concentrations of another ligand so that a complete two-dimensional array of substrate and effector concentrations was examined. In some cases, additional parameters were introduced into the coupling interaction by varying the concentration, solution pH, or temperature of another ligand. Generally, assays to characterize the coupling in the presence of MgATP (i.e., catalysis) were done using steady-state kinetics, and assays in the absence of MgATP (i.e., strictly binding) were done using steady-state fluorescence emission. For some activity assays performed under subsaturating concentrations of MgATP, the decrease in the absorbance value that was attributed to the oxidation of NADH and that correlated with PFK activity was close to the limit of instrumental detection. We adopted another coupling method in which the change in absorbance due to the oxidation of NADH is produced by the conversion of pyruvate to L-lactate. In this coupling scheme, MgATP is directly and efficiently recycled using pyruvate kinase (70 μg) and lactate dehydrogenase (70 μg). Thus, the addition of even minute concentrations of MgATP reflects a constant amount throughout the duration of the reaction. The amount of PEP (1 mM) added to push the reaction forward does not interfere with the amount of PEP added as the independent variable, because the reaction never proceeds to a significant extent. Most activity curves were carried out using a Beckman DU640 spectrophotometer from which changes in absorbance per unit time were measured. PFK was appropriately diluted so that the introduction of 5 μL of PFK into a 1-mL reaction mixture gave an approximate absorbance change of $0.005 < A < 0.3$ in 5 min.

Steady-State Fluorescence Measurements. Fluorescence emission intensity and anistropy were measured as described previously (*7*).

Data Analysis. The notations adopted here for data analysis have been thoroughly described (*7*, *8*, *16*): a = Fru-6-P, b = MgATP, and y = PEP. For kinetic analysis, we assumed that either the substrate or the effector ligand achieved a near-binding equilibrium in the time course of the steady-state assay so that the $K_{1/2}$ (enzymatically determined constant, K_a) approximates the dissociation constant K_{ia} (*14*, *17*, *18*). This assumption has been shown to be valid for Fru-6-P but not for MgATP ($K_{ib} \cong 0.025$ μM and $K_b = 50$ μM). However, the expression is still valid if one of the ligands in the interaction achieves equilibrium, as has been thoroughly discussed by others (*13*, *19*). The binding of two substrates (A and B) and one allosteric ligand (Y), each to a distinct site, is given by the rate equation (*20*):

$$\nu/E_T = V^\circ(K^\circ_{iy}Q_{ab}[A][B] + Q_{aby}[A][B][Y])/(K^\circ_b K^\circ_{iy}[A] + K^\circ_a K^\circ_{iy}[B] + K^\circ_a K^\circ_b[Y] + K^\circ_{iy}Q_{ab}[A][B] + K^\circ_b Q_{ay}[A][Y] + K^\circ_a Q_{by}[B][Y] + Q_{aby}[A][B][Y] + K^\circ_a K^\circ_b K^\circ_{iy}) \quad (1)$$

where V° is the maximal rate and K°_{ia} and K°_{iy} are the dissociation constants for the substrate and allosteric effector, respectively, in the absence of any other ligand. The coupling constant Q (Q_{ay}, Q_{ab}, Q_{by}, or Q_{aby}) describes the limit of the allosteric effects on binding affinity. Equation 1 stipulates that the presence of both substrates is essential for turnover to occur. A complete three-dimensional matrix of K_a values at given concentration ranges of MgATP and PEP is expressed by (*16*)

$$K_a = \frac{K^\circ_b}{K^\circ_a K_b}\left[\frac{(K^\circ_{iy} + Q_{ay}[Y]) + (K^\circ_{iy} + Q_{by}[Y]) + ([Y] + K^\circ_{iy})}{(K^\circ_{iy}Q_{ab} + Q_{aby}[Y])}\right] \quad (2)$$

A two-ligand coupling interaction can be determined when the concentration of a third ligand is nonzero. The following expression, derived from eq 1, can be used to examine purely *K*-type effects where $W = 1$ (*13*, *14*, *21*):

$$K_a = K^\circ_{ia}\left(\frac{K^\circ_{iy} + [Y]}{K^\circ_{iy} + Q_{ay}[Y]}\right) \quad (3)$$

where K_a (or an analogous enzymatically determined $K_{1/2}$) represents the apparent substrate concentration at half-fractional saturation. The interaction of two substrates and one allosteric ligand was evaluated using an expression similar in form to eq 3. Reinhart has shown that derivation of the rate equations to measure multiple ligands binding to the enzyme takes on forms similar to those of eq 1 (*10*, *13*, *16*). Thus, for *K*-type effects, the coupling parameters can be derived from equations similar to eq 2. For each set of K_a values measured when the MgATP concentration is zero, the K_a, K_{iy}, and Q_{ay} are obtained, as shown in eq 2. When the concentration of MgATP is above zero, the K'_a, K'_{iy}, Q'_{ab}, and Q'_{by} are described by

$$K'_a = K'^\circ_a\left(\frac{K'^\circ_b + [B]}{K'^\circ_b + Q'_{ab}[B]}\right) \quad (4)$$

where a prime symbol denotes the value measured when the concentration of the third parameter (in this case, y or PEP) is nonzero. When Fru-6-P is present, the coupling expression for MgATP and PEP is determined by

$$K'_{iy} = K'^\circ_{iy}\left(\frac{K'^\circ_b + [B]}{K'^\circ_b + Q'_{by}[B]}\right) \quad (5)$$

and

$$Q'_{ay} = \frac{(K^\circ_b + Q_{ab}[B])(K^\circ_b + Q_{by}[B])}{(K^\circ_b + [B])(K^\circ_b Q_{ay} + Q_{aby}[B])} \quad (6)$$

For purely *V*-type effects, the expression was determined by

$$V_{max} = V_a\left(\frac{K^\circ_{iy} + W_{ay}[Y]}{K^\circ_{iy} + [Y]}\right) \quad (7)$$

$$V_a = V^\circ_a\left(\frac{K^\circ_b + W_{ab}[B]}{K^\circ_b + [B]}\right) \quad (8)$$

and

$$W_{ay} = \frac{K^\circ_{iy}W_{ab} + W_{aby}[Y]}{K^\circ_{iy} + [Y]} \quad (9)$$

where V_{max} is the observed maximal rate, V°_a is the maximal rate for Fru-6-P when the concentration of PEP equals zero, and W_{ay} represents V^∞/V° (i.e., a ratio of the maximal rate for Fru-6-P when PEP is saturating to that of Fru-6-P when PEP is absent). Note the equations above express the binding of three ligands to a monomeric enzyme. For a multisubunit enzyme, such as PFK, the multiple binding events for each ligand are assumed to be equivalent. The expressions above are thus relevant for the dissociation constants and coupling parameters describing the macroscopic averages of these events.

The Gibbs free energy expressions to describe the coupling interaction between the substrate and ligand in the absence and presence of MgATP are

$$\Delta G_{ay} = -RT\ln(Q_{ay}) = \Delta H_{ay} - T\Delta S_{ay} \quad (10)$$

and

$$\Delta G_{ay/b} = -RT\ln(Q_{ay/b}) = \Delta H_{ay/b} - T\Delta S_{ay/b} \quad (11)$$

Equations were written into Kaleidagraph (Synergy Software, Reading, PA) and fit using a 7100 Power PC Macintosh.

RESULTS

Quantification of the Fru-6-P/PEP Coupling Interaction in Saturating Concentrations of MgATP. Enzymatic assays of PFK were performed at 3 mM MgATP and at various concentrations of Fru-6-P and PEP. The resultant *K*- and *V*-type effects of PEP on the binding of Fru-6-P to the E187A mutant PFK enzyme are shown in Figure 1. When PEP was absent, Fru-6-P displayed a sigmoidal isothermal profile with a Hill coefficient of 3.2 and a $K_{1/2}$ of 1.8 mM. Increasing the PEP concentrations resulted in a reduction in the maximal turnover rate, a transformation from a sigmoidal to a hyperbolic profile, and a left shift of the substrate concentration at half-V_{max} for Fru-6-P. The maximal turnover rate decreased by 5% at 0.1 mM PEP, by 20% at 4 mM PEP,

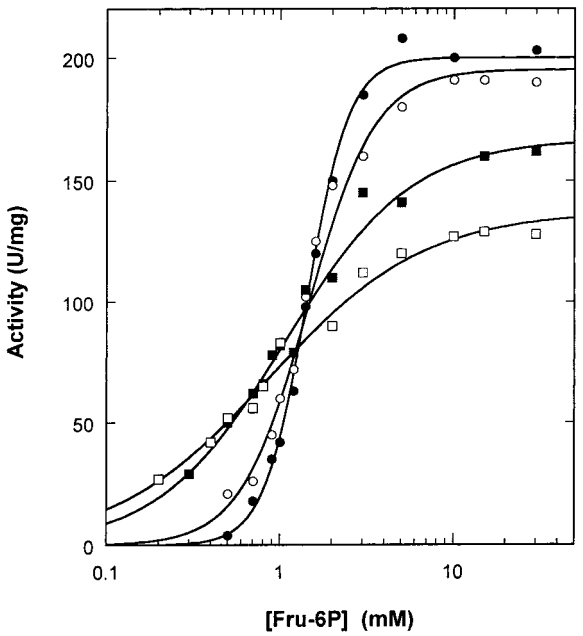

FIGURE 1: Dependence of the steady-state enzymatic activity for the E187A mutant PFK of Fru-6-P in the presence of 0 (●), 0.1 (○), 4 (■), and 30 (□) mM PEP. Activities were determined by coupling the PFK reaction to the oxidation of NADH and observing the absorbance change at 340 nm. Each rate profile was analyzed using the Hill equation. The solid lines represent the nonlinear regression fit. The experiment was performed in 50 mM EPPS−KOH, 10 mM $MgCl_2$, and 100 mM KCl at pH 8 and 25 °C.

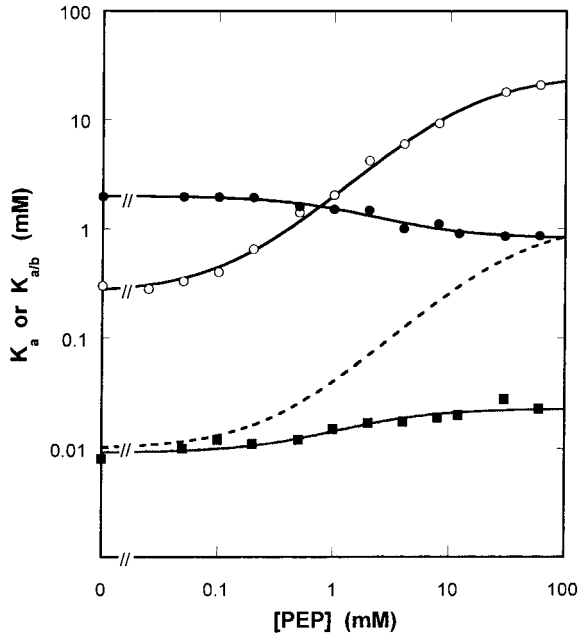

FIGURE 2: Dependence of the equilibrium constant for Fru-6-P ($K_{a/b}$) as a function of PEP in the wild-type (○) and the mutant E187A enzymes (●). $K_{a/b}$ was determined from enzymatic assays in which MgATP was present in the saturating concentration of 3 mM. Each $K_{a/b}$ determination was derived from a Hill equation fit of data comprising 10−12 activity measurements at a constant PEP concentration. The solid lines represent fits to eq 3. Dependence of the dissociation constant for Fru-6-P (K_a) as a function of PEP in the absence of MgATP in the E187A mutant is represented by (■). The same interaction for the wild-type enzyme has been previously determined and is represented by the dashed line. Changes in the fluorescence emission intensity were monitored either from 10-s integrations at 350 nm or from emission scans of 310−500 nm. Measurements were performed in buffer conditions similar to those of the kinetic assays minus the components essential for catalysis measurement. Each data point represents the result from a Michaelis−Menton fit of a binding profile consisting of 12−15 Fru-6-P concentrations.

and by 40% at ≥60 mM PEP. However, no effector ligand is known to exert influence on the maximal rate of activity of the wild-type enzyme. The change from a sigmoidal to a hyperbolic profile in the mutant enzyme was indistinguishable from that in the wild-type counterpart and indicates that MgATP induced homotropic cooperativity in Fru-6-P. Increasing the PEP concentration to 30 mM led to a decrease in $K_{1/2}$ from an initial value of 1.8 mM to 1 mM, resulting in an increased binding affinity and a decreased maximal rate. Consistent with reports from Lau and Fersht (*1*, *2*), these data indicate that the E187A mutation converted the role of PEP from solely a *K*-type inhibitor to both a *K*-type activator and a *V*-type inhibitor of Fru-6-P binding to PFK.

K- and *V*-type effects were quantified from the dependence of $K_{1/2}$ and V_{max}, respectively, as functions of PEP concentration. Figure 2 shows the variation in $K_{1/2}$ (or K_a) of Fru-6-P for the wild-type and the E187A mutant enzymes. Fit of these data to eq 3 gives values for Q_{ay}, K_a (or $K_{1/2}$), and K°_{iy}. The $K_{a/b}$ value for Fru-6-P in the wild-type enzyme increased from 0.3 mM in zero PEP concentration to 11 mM in 60 mM PEP, giving a $Q_{ay/b}$ value of 0.01. The 0.011 coupling value in the presence of a saturating concentration of MgATP indicated a 90-fold inhibition of the interaction between the Fru-6-P and PEP. In contrast, the $K_{1/2}$ for the E187A mutant shifted downward from 1.8 ± 0.04 to 0.9 ± 0.1 mM upon approaching saturating concentrations of PEP. The effect was a modest 2-fold activation ($Q_{ay/b}$ = 2.0 ± 0.1). The diametrical trends of the PEP-dependent $K_{1/2}$ values between the wild-type and the E187A mutant forms suggest major changes in the nature of allosteric actions resulting from the E187A mutation at the allosteric site. Trends in $K^{\circ}_{ix/b}$, the dissociation constant for PEP, were comparable to those in the wild-type enzyme throughout the range of Fru-6-P concentrations examined (data not shown).

Quantification of Fru-6-P/PEP Coupling in the Absence of MgATP. The coupling interaction of Fru-6-P and PEP in the absence of MgATP was measured by fluorescence emission. As is the case for most three-ligand interactions characterized for the wild-type enzyme (*8*, *9*), multiple ligands produced fluorescence alterations distinct from the signal each ligand produced when independently introduced to the protein. The unique fluorescence signal suggests that the saturation plateau consists mainly of the ternary complex, rather than a substrate molecule "bumping" an inhibitor molecule to form another binary complex as predicted by two-state theories. Although the E187A mutation did not affect the fluorescence properties of ligands interacting at the active site of the enzyme, the mutation did alter the fluorescence properties of all ligands interacting at the allosteric site, both in the absence and in the presence of other ligands (*7*). For both the wild-type and the E187A mutant PFK, a saturating amount of Fru-6-P reduced the emission intensity by approximately 28%. Trp 311 was unresponsive to the binding of PEP in the mutant enzyme but produced a 13% increase in the emission intensity in the wild-type enzyme. Likewise, MgADP produced no changes in emission intensity for the E187A mutant but did cause a 28% reduction for the wild-type enzyme. Although PEP alone did not produce changes in the tryptophanyl fluorophore, the presence of PEP lessened the amplitude of

quenching by Fru-6-P. The amplitude for Fru-6-P decreased as a function of PEP in a hyperbolic manner, giving an initial value of 28% in the absence of and a final value of 15% in the presence of saturating PEP concentrations.

Figure 2 compares the dependence of the equilibrium constant for Fru-6-P as a function of PEP in the absence versus the presence of 3 mM MgATP. Differences in the initial K_a and $K_{a/b}$ values for Fru-6-P (in the absence of PEP) indicated linkage exists between the substrates and, with $K_{a/b}$ higher than K_a, there is considerable antagonism between Fru-6-P and MgATP. Fru-6-P bound to the free PFK mutant with an affinity comparable to that in the wild-type enzyme ($K^{\circ}_{ia} = 12\ \mu$M) (*8*). However, after MgATP was added, the initial K_{ia} value shifted sharply upward to approximately 2 mM. The magnitude of this antagonism was more striking in the mutant than in the wild-type enzyme; MgATP reduced Fru-6-P affinity by approximately 30-fold (*8*) in the wild-type enzyme, compared with 300-fold in the mutant.

The Fru-6-P/PEP coupling interaction in the absence of MgATP directly contrasted with coupling in the presence of MgATP. In the presence of identical buffer solutions excluding MgATP and other components necessary to measure catalysis, PEP displayed a modest 2-fold inhibition toward the binding of Fru-6-P to the mutant enzyme. The very same interaction yielded a 90-fold antagonistic effect on Fru-6-P binding in the wild-type enzyme, causing a net 2-fold augmentation of the inhibitory effect on the coupling of Fru-6-P and PEP (*8*). The influence of MgATP accounts for this difference between the mutant and the wild-type enzymes. Like the wild-type enzyme, the E187A mutant exhibited an inhibition pattern that indiated the onset of a saturation plateau at high PEP concentrations, revealing that the pattern was not the result of the mutually exclusive binding between PEP and Fru-6-P. The converging trends reveal the antithetical nature of allosteric actions by PEP—one inhibiting and the other activating—that are imposed conditionally by MgATP.

Role of MgATP in the Fru-6-P/PEP Coupling Interaction. Because the coupling between Fru-6-P and PEP was activating in the presence and inhibiting in the absence of MgATP, varying the MgATP concentrations revealed the "crossover" point from activation to inhibition. Fru-6-P/PEP enzymatic coupling assays were performed with MgATP concentrations fixed at some constant range of 0.01−3 mM. At zero concentration MgATP, the coupling interaction was monitored by fluorescence emission intensity. For each particular MgATP concentration examined, the concentration of PEP was varied from 0.05 to 60 mM and Fru-6-P from 0.05 to 20 mM. The maximal rate of activity was approximately 200 units/mg at ≥3 mM MgATP. The rate decreased correspondingly at lower MgATP concentrations. At 0.2 mM MgATP, the activity decreased by 50%. At concentrations <0.1 mM MgATP, Fru-6-P exhibited higher binding affinities. Owing to technical difficulties in monitoring absorbance changes, enzymatic assays at MgATP concentrations <10 μM were not performed.

The Hill coefficient appears to be unaffected by MgATP concentrations in the range of 0.01−3 mM, considering that MgATP induces Fru-6-P cooperativity. The $K_{1/2}$ and V_{max} values from each binding profile generated from fits were then fit to eqs 3 and 7, respectively. Data fit of the apparent $K_{1/2}$ values for Fru-6-P as a function of PEP yielded three

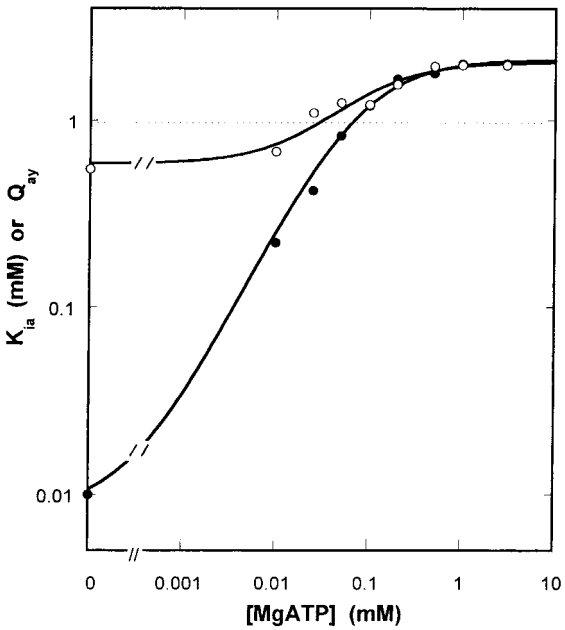

FIGURE 3: Equilibrium parameters describing the Fru-6-P/PEP coupling interaction as a function of MgATP concentration. For each MgATP concentration, the dependence of K_a for Fru-6-P upon the addition of PEP was fit to eq 3 to derive K°_{ia}, K°_{iy}, , and Q_{ay}. The reaction of 3 mM MgATP is shown in Figure 2. K°_{iy} (not shown) remained constant throughout the range of MgATP concentrations examined. The dependence of K°_{ia} for Fru-6-P as a function of MgATP is shown by (●). The solid line represents the fit of the data to eq 4 to obtain K'°_{ib} for MgATP and Q'_{ab} for Fru-6-P/MgATP. The dependence of the coupling constant Q_{ay} on MgATP is shown by (○), with the solid line representing the fit to eq 6.

dependent patterns: the K°_{ia} values for Fru-6-P in the absence of any other ligand, K°_{iy} for PEP in the absence of Fru-6-P, and the coupling constant Q_{ay} describing the effects of MgATP on the interaction between Fru-6-P and PEP. K°_{iy} constants for PEP appeared to be unchanged throughout the range of MgATP concentrations examined, with values fluctuating around 1.2 ± 0.5 mM (data not shown). The dependence of K°_{ia} and Q_{ay} on varying concentrations of MgATP for the E187A mutant PFK are shown in Figure 3. K°_{ia} initiated at around 0.008 mM in zero MgATP concentration, increased in a saturable manner, and approached a plateau of approximately 2 mM at high MgATP concentrations. Although a similar pattern of increase was observed for the wild-type enzyme, the inhibition by MgATP was less effective (~0.008−0.5 mM) than in the mutant. Fit of data to eq 4 revealed an inhibition magnitude of approximately 300-fold. The mutual influence of Fru-6-P and PEP was reinforced by approximately 2-fold in saturating concentrations of MgATP and diminished with lowering MgATP concentrations to approach an abolishment of allosteric influence at 25 μM. This MgATP concentration represents the crossover point from activation to inhibition, with activation above and inhibition below 25 μM. The Q_{ay} coupling value is 1.08 ± 0.04 at 25 μM MgATP, decreasing to 0.7 ± 0.1 at 10 μM and approaching a final value of 0.5 ± 0.03 at zero concentration MgATP. The magnitude of inhibition, a modest 2-fold, is comparable to the amplitude of activation. The results indicate that the mutually linked interaction between Fru-6-P and PEP, giving rise to either *K*-type activation or K-type inhibition, depends on the concentration of MgATP.

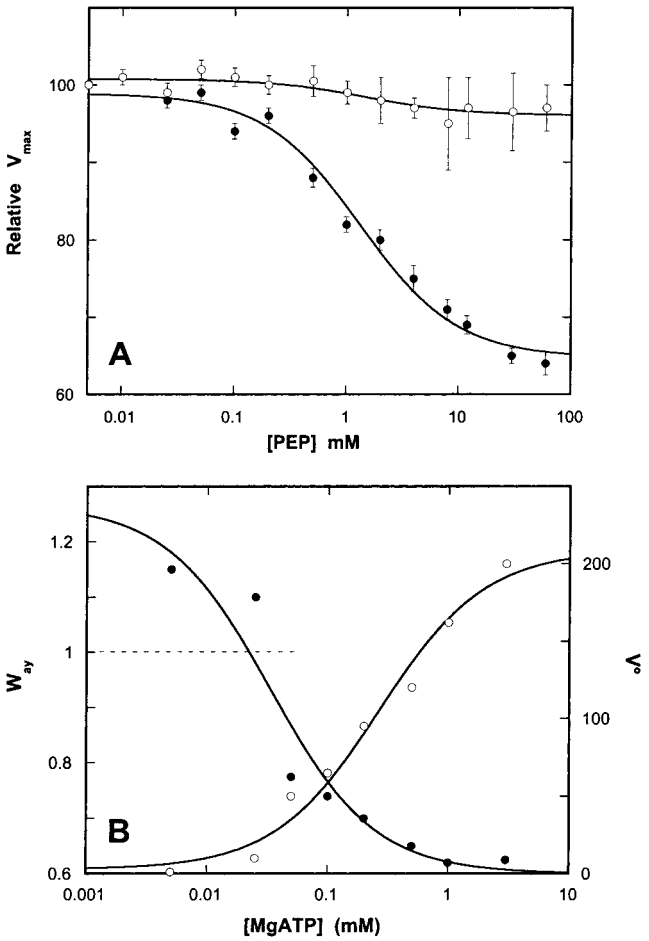

FIGURE 4: (A) Variation in the maximal activity of Fru-6-P as a function of PEP for the wild-type (○) and the mutant E187A (●) PFK. Each V_{max} value was derived from a fit to the Hill equation. The solid lines represent the fits to eq 7. The assay was carried out in the presence of a saturating concentration of MgATP (3 mM) at pH 8 and 25 °C. (B) Variations in coupling parameters representing the maximal activity for the interaction of Fru-6-P and PEP as a function of MgATP. Each data point represents the fit of the maximal profile for Fru-6-P (represented in panel A) to yield the V°, K°_{iy}, and W_{ay}. K°_{iy} values for PEP (not shown) remained invariant throughout the range of MgATP concentrations used. The dependence of the V° parameter for Fru-6-P as a function of MgATP concentration is represented by (○), with the solid line representing the fit to eq 8. The variation of W_{ay} as a function of MgATP is represented by (●), with the solid line representing the fit to eq 9.

The Influence of MgATP on the Maximal Rate of Activity. Figure 4A shows the corresponding variation of V_{max} for Fru-6-P at the PEP concentration ranges given above. Saturating concentrations of MgATP were maintained. The wild-type enzyme did not exhibit significant changes in the maximal rate of activity at PEP concentrations of 0−60 mM ($W = 0.9 \pm 0.1$). However, the mutant displayed up to a 40% decrease at PEP concentrations approaching 60 mM. The decrease in V_{max} from 190 ± 1.8 to 121 ± 4 units/mg with increasing PEP concentrations denoted a 1.5-fold inhibition of the maximal turnover rate ($W = 0.6 \pm 0.03$) (Figure 4A). Also, the inhibition in the E187A mutant PFK appeared to decrease, but not completely disappear, at lower temperatures (data not shown). The W value approached 0.8 ± 0.06 at 5 °C and accompanied by an increase in the K°_{iy} for PEP. The W parameter also appeared to exhibit a relatively minor change throughout the pH range of 5−10, decreasing to approximately 0.3 in acidic conditions (data not shown).

Table 1: Dissociation Constants for Fru-6-P, or PEP, or MgATP

ligand	other saturating ligand	designation	dissociation constant (mM)
Fru-6-P		K°_{ia}	0.009 ± 0.001
	MgATP	$K^\circ_{ia/b}$	1.8 ± 0.2
	MgATP, PEP	$K^\circ_{ia/x1}$	0.9 ± 0.1
	$MgADP_{(eff)}$	$K^\circ_{ia/x2}$	0.015 ± 0.001
	$MgADP_{(act)}$	K°_{ix}	0.1 ± 0.03
	$MgADP_{(eff)}$, MgATP, PEP	$K^\circ_{ix/bx1}$	1.6 ± 0.02
PEP		K°_{ix}	0.3 ± 0.02
	Fru-6-P	$K^\circ_{ix/y}$	1.3 ± 0.4
	Fru-6-P, MgATP	$K^\circ_{ix/ab}$	1.7 ± 0.3
	MgATP	K°_{ix2}	1.4 ± 0.2
	MgADP, MgATP	$K^\circ_{ix2/a}$	3.1 ± 0.2
MgATP		$K^\circ_{ia/x1}$	0.0003 ± 0.00001
	Fru-6-P	$K^\circ_{ia/x1}$	0.04 ± 0.01

MgATP also mitigated the inhibition of the maximal turnover rate. The V_{max} limits for Fru-6-P as a function of PEP were determined at a range of fixed MgATP concentrations. The resultant parameters from eq 8 fits for each nucleotide concentration are shown in Figure 4B. The K°_{iy} values remained virtually unchanged throughout the range of MgATP concentrations (data not shown). Because MgATP is necessary for catalysis, the Fru-6-P turnover rate was, predictably, enhanced at increasing MgATP concentrations. The rate of turnover was <20 units/mg in micromolar concentrations of MgATP, increasing to 200 ± 4 units/mg at 3 mM.

The coupling constant describing the maximal rate of activity, W_{ay}, seemed to show crossover effects that were also dependent on MgATP (Figure 4B). An apparent inhibition of the maximal rate of activity occurred at MgATP concentrations >50 μM ($W < 1$). The inhibition magnitude is mitigated at decreasing MgATP concentrations and is activated at concentrations <35 μM ($W > 1$). Interestingly, the *V*-type crossover from inhibition to activation occurred in the same MgATP concentration range that invoked *K*-type crossover. These crossover trends appear antithetical, such that decreasing MgATP concentrations simultaneously cause *K*-type inhibition and *V*-type activation. We are uncertain whether these MgATP-concentration-dependent crossovers are related coincidentally or whether they imply that the underlying mechanisms of *K*- and *V*-type effects are linked.

Table 1 summarizes the dissociation constants for Fru-6-P, MgATP, and PEP, each of which participates in the individual binding and coupling interactions. A comparison of these values from previous reports (*7*−*9*) verified that the equilibrium constants for each ligand when all other ligands are absent in the E187A mutant are nearly identical to those in the wild-type enzyme. However, the presence of a second or a third ligand yielded values substantially different from those reported for the wild-type enzyme (*7*−*9*). Table 2 summarizes the coupling parameters for combinations of substrate and effector ligand interactions. The coupling values indicated that most two- or three-way interactions were substantially weaker in the E187A mutant than in the wild-type *E. coli* PFK (*8*). One exception was the inhibitory coupling between Fru-6-P and MgATP, which was approximately 5-fold more potent in the mutant than in the wild-type PFK. The coupling interactions between MgATP and PEP were comparable in the two enzyme forms. The results suggest that the mutation predominately affects the

Table 2: Coupling Parameters Quantifying the Possible *K*- and *V*-Type Interactions between Fru-6-P and Other Ligands for the E187A Mutant PFK

coupled ligand	other saturating ligand	designation	coupling constant
Fru-6-P/PEP		Q_{ay}	0.5 ± 0.03
	MgATP	$Q_{ay/b}$	2.0 ± 0.1
	MgATP, MgADP	$Q_{ay/bx}$	1.9 ± 0.5
PEP/MgATP		Q_{ay}	1.9 ± 0.4
	Fru-6-P	$Q_{by/a}$	3.7 ± 0.4
Fru-6-P/MgATP		Q_{ab}	0.003 ± 0.001
	PEP	$Q_{ab/y}$	0.01 ± 0.004
Fru-6-P/MgATP/PEP		Q_{aby}	0.006 ± 0.002
Fru-6-P/PEP	MgATP	$W_{ay/b}$	0.7 ± 0.03
Fru-6-P/MgATP		W_{ab}	1.3 ± 0.06
Fru-6-P/MgATP/PEP		W_{aby}	0.6 ± 0.02

interaction between multiple ligands rather than the binding affinities of any individual ligand.

Shift in Thermodynamic Mechanisms Governing the Fru-6-P/PEP Coupling Interaction. Temperature dependence studies provide strong evidence that the E187A mutation alters predominately the coupling interactions. All van't Hoff analyses of the wild-type and the E187A mutant for the Fru-6-P/PEP couplings in the presence and absence of MgATP showed linearly dependent couplings, indicating that the values of enthalpy remained constant over the temperature range examined. However, other features of the temperature-dependent patterns of the mutant connote significant deviations from the wild-type enzyme. The E187A mutation reduced the slope of a linearly dependent pattern, reflecting an overall loss of 3 kcal/mol of the enthalpic contribution. Both Fru-6-P/PEP interactions in the presence and absence of MgATP for the E187A mutant are severely weakened, as indicated by the extreme upward repositioning of the linear patterns. The *Q* dependence on temperature implies that MgATP shifts the overall linear pattern upward. For the wild-type enzyme, this upward shift led to an approximately 2-fold mitigation of the antagonistic interaction. For the E187A mutant, MgATP caused the already weakened inhibitory Fru-6-P/PEP interaction to switch to activation. These results indicate that the mutation induces a moderate loss of the enthalpic contribution, thus causing the weakened Fru-6-P/PEP coupling interaction to be driven mainly by entropy.

Table 3 summarizes the contribution of the enthalpic and entropic components to the Fru-6-P/PEP coupling in the presence and absence of MgATP. In all instances of couplings, whether activating (given by negative ΔG) or inhibiting (given by positive ΔG), the ΔH and ΔS for the Fru-6-P/PEP and Fru-6-P/PEP/MgATP are of the same sign. This finding indicates that the component energetic forces compete, causing a net cancellation of the enthalpic and entropic terms. The resultant effect is a small contribution by the coupling free energy of <2 kcal/mol toward the reaction. MgATP does not cause a severe alteration in coupling free energy in the mutant but has a greater impact on the constituent enthalpic and entropic components. The magnitude of the ΔH and ΔS in the mutant reveals that Fru-6-P/PEP coupling without MgATP remains enthalpically driven but becomes entropically dominated when MgATP is present. For the wild-type enzyme, this contribution by MgATP is not enough to shift the enthalpically dominated interaction to an entropically driven one but does mitigate the inhibitory effects of the ligands on each other. The same contribution by MgATP tips the balance of energetics in a weak coupling interaction, causing the ΔH term to overcome the entropic forces.

Contribution of MgATP to the Total Coupling Enthalpic and Entropic Components. Table 3 quantitatively compares the net contributions by MgATP to thermodynamic coupling parameters for the Fru-6-P/PEP interactions between the wild-type and E187A mutant enzymes. For both enzyme species, MgATP appears to contribute substantially to the total coupling entropic and enthalpic components. MgATP contributed a *positive* 8 kcal/mol each of ΔH and ΔS to the Fru-6-P/PEP coupling energetics for the wild-type enzyme, providing approximately 50% of the total. In contrast, the action by MgATP toward the E187A mutant contributed a *negative* 5 kcal/mol each of ΔH and $T\Delta S$, which represented a greater proportion of the total energetics of the coupling ($\geq 80\%$). The opposing signs of the constituent thermodynamic terms between the mutant and the wild-type enzyme resulted in a common end point, a minor activating (or rather an attenuation of the inhibitory) effect between Fru-6-P and PEP. The net result of this switch in thermodynamic signs by MgATP is the activation of Fru-6-P/PEP coupling. The positive ΔH and ΔS yield a net -0.3 kcal/mol of the coupling free energy, which somewhat reduces the inhibitory effects of PEP toward Fru-6-P. This mitigation of inhibition is inconsequential in the wild-type enzyme, because the coupling between Fru-6-P and PEP itself is strong ($Q_{ay/b} = 0.011$, 90-fold inhibition). Because the E187A mutation considerably weakens the coupling ($Q_{ay/b} = 2.0 \pm 0.1$, 2-fold activation), the contribution of approximately 1 kcal/mol to the negative ΔH and ΔS in the conditional presence of MgATP tips the balance from inhibition to activation. The difference in the thermodynamic contribution of the wild-type versus that of the E187A mutant—approximately 14

Table 3: Thermodynamic Parameters for the Fru-6-P/PEP Coupling Interactions in the Presence and Absence of MgATP for Wild-Type and E187A Mutant PFK

Fru-6-P/PEP or Fru-6-P/PEP/MgATP		ΔG (kcal/mol)	ΔH (kcal/mol)	ΔS (kcal/mol) (298 K)
wild type	Q_{ay}	$+2.7 \pm 0.1$	$+9.1 \pm 1.3$	$+6.4 \pm 1.3$
	$Q_{ay/b}$	$+2.4 \pm 0.2$	$+17.2 \pm 1.8$	$+14.8 \pm 1.8$
	$Q_{ay/b}/Q_{ay}$	-0.3 ± 0.1	$+8.1 \pm 0.5$	$+8.4 \pm 0.5$
mutant E187A	Q_{ay}	$+0.6 \pm 0.4$	$+6.6 \pm 0.4$	$+6.0 \pm 0.4$
	$Q_{ay/b}$	-0.3 ± 0.2	$+0.8 \pm 0.3$	$+1.1 \pm 0.1$
	$Q_{ay/b}/Q_{ay}$	-0.9 ± 0.2	-5.8 ± 0.1	-4.9 ± 0.3
	$Q_{ay/b}/Q_{ay}$ (wild-type)/$Q_{ay/b}/Q_{ay}$ (E187A)	-0.6 ± 0.2	-13.9 ± 0.4	-13.3 ± 0.2

kcal/mol—suggests that the mutation substantially alters the energetic components contributed by MgATP.

DISCUSSION

Site-specific mutation of Glu 187 appears to alter predominately the coupling interactions between multiple ligands. The binding affinity of each ligand, Fru-6-P, PEP, or MgADP, to the PFK enzyme was not significantly affected by the mutation. When all other ligands are absent, each ligand in the mutant binds with an affinity comparable to that of the wild-type enzyme. However, the presence of a second or third ligand in the mutant causes a profound change in the binding affinity of the bound ligand. MgATP lowers the binding affinity of Fru-6-P by approximately 300-fold, compared with a 30-fold reduction in the wild-type enzyme. MgADP loses its allosteric influence toward Fru-6-P (*7*). PEP is inhibitory toward Fru-6-P when MgATP is absent but becomes activating when MgATP is present. One coupling that does not appear to be affected by the mutation is the competition of MgADP with MgATP for binding at the active site. Also, PEP and MgATP have little influence on each other's binding. However, the activation by PEP in the E187A mutant depends on the presence of MgATP, which indicates that MgATP greatly influences the Fru-6-P/PEP coupling.

Consistent with our previous findings (*9*, *22*−*24*), the sign of coupling ΔH and ΔS is the same, regardless of whether the coupling is activating or inhibiting. Because entropy and enthalpy oppose one another and the coupling free energy represents the difference between ΔH_{ay} and $T\Delta S_{ay}$, the term with the greater absolute value drives the coupling interaction. In the wild-type enzyme, the main driving force for the Fru-6-P/PEP coupling is enthalpic; mutation at position 187 causes the coupling between Fru-6-P and PEP to become entropically driven. Couplings for other triply mutated enzyme forms that include the E187A mutation also show changes from enthalpically to entropically driven coupling (unpublished data). The switch from inhibition to activation coincides with the changes in the entropy-dominated role. However, because both activation and inhibition occur in other entropy-dominated systems (*17*, *23*, *25*) the relationship between the allosteric effect and the thermodynamic components is not explicit.

The same sign for enthalpy and entropy terms indicates a net cancellation of competing individual thermodynamic components. The binding of a ligand to a localized site on the enzyme causes structural perturbations such that the energy in the protein increases in some areas and decreases in others. The enthalpic change may be attributable to protonation reactions or to bond formations and disruptions. The contribution of entropy may result from the rearrangements of the water molecules around the protein structure or from side-chain perturbations. More than one of these processes can operate concurrently, leading to a cancellation of their respective contributions to the energetics and a small net effect on the resultant coupling energy. Activation and inhibition result from many such interactions and lie on a continuum in which the environment dictates the extent and nature of regulation. The increase in entropy that occurs during the conformation change can be compensated for by an increase in enthalpy that results from the interaction and by a decrease in the entropy of other regions of the protein. The net effect of compensation is a lowered ΔG_{ay} of interaction. The ΔG_{ay} for the overall coupling is approximately 2 kcal/mol or less, a value that is experimentally and biophysically consistent with our results and those obtained in several systems examined (*8*, *9*, *26*). The small magnitude of the coupling parameter reflects an inherently weak coupling between an allosteric ligand and its substrate, and transitions between activation and inhibition are possible. In addition, most of the compensation behavior manifested in linked systems are based on weakly coupled interactions—an inherent characteristic of biological systems. Since the efficacy of enzyme catalysis requires that substrates and effectors readily bind and more easily dissociate in response to need, the dissociation constants within the micromolar to millimolar range are associated with weak couplings. Also, individual free energy of binding for each kinetic step occurs at values >10 kcal/mol, but the free energies of the coupling interaction, as derived from linkage, occur at values of approximately 2 kcal/mol. The <2 kcal/mol value is equivalent to the breakage of a single hydrogen bond, to the formation of an ionic bond, or to the loss of a hydrophobic interaction in the absence of other steric effects.

A rigorous thermodynamic linkage model allowed us to observe crossover phenomena. In *Bacillus stearothermophilus*, the allosteric effect of MgADP changes at 16 °C, resulting in the activation of Fru-6-P above and inhibition below this temperature (*27*). Inositol monophosphate, an inhibitor for *E. coli* carbamoyl phosphate synthetase, reverses its effects on MgADP binding at 37 °C (*27*). The coupling between MgATP and PEP activates Fru-6-P above and inhibits Fru-6-P below 35 °C in the wild-type *E. coli* PFK (*8*). Owing to experimental and framework restrictions, crossover phenomena are rarely reported by others. For example, Uyeda and Racker have reported the loss of allosteric effects at pH 8 in rabbit muscle PFK, in which MgATP is an efficacious inhibitor in the higher protonated environment (*28*). However, experiments to determine whether activation occurs were not performed at pH values >8. The Bohr effect in horse myoglobin and human hemoglobin has been shown to undergo a reversal in response to extreme pH and ionic strength (*29*). The effect of NaCl on the activity of γ-thrombin amidase, a digested portion of human thrombin, as a function of pH yields two crossover points, an enhancement in the binding affinity below pH 7 and above pH 9.7 and an inhibitory interaction between these pH values (*30*). Our results show that the balance between inhibition and activation depends on the availability of a threshold concentration of MgATP.

REFERENCES

1. Lau, F. T.-K., and Fersht, A. R. (1987) *Nature 326*, 811−812.
2. Lau, F. T.-K., and Fersht, A. R. (1989) *Biochemistry 28*, 6841−6847.
3. Auzat, I., Le Bras, G., Branny, P., De La Torre, F., Theunissen, B., and Garel, J. R. (1994) *J. Mol. Biol. 235*, 68−72.
4. Shirakihara, Y., and Evans, P. R. (1988) *J. Mol. Biol. 204*, 973−994.
5. Evans, P. R., Farrants, G. W., and Hudson, P. S. (1981) *Philos. Trans. R. Soc. London, Ser. B 293*, 53−62.
6. Schirmer, T., and Evans, P. R. (1990) *Nature 343*, 140−145.

7. Pham, A. S., Janiak-Spens, F., and Reinhart, G. D. (2001) *Biochemistry 40*, 4140−4149.
8. Johnson, J. L., and Reinhart, G. D. (1997) *Biochemistry 36*, 12814−12822.
9. Johnson, J. L., and Reinhart, G. D. (1994) *Biochemistry 33*, 2635−2643.
10. Johnson, J. L., and Reinhart, G. D. (1992) *Biochemistry 31*, 11510−11518.
11. Deville-Bonne, D., and Garel, J.-R. (1992) *Biochemistry 31*, 1695−1700.
12. Johnson, J. L., and Reinhart, G. D. (1994) *Biochemistry 33*, 2644−2650.
13. Reinhart, G. D. (1983) *Arch. Biochem. Biophys. 224*, 389−401.
14. Reinhart, G. D. (1988) *Biophys. Chem. 30*, 159−172.
15. Kotlarz, D., and Buc, H. (1977) *Biochim. Biophys. Acta 484*, 35−48.
16. Braxton, B. L., Mullins, L. S., Raushel, F. M., and Reinhart, G. D. (1999) *Biochemistry 38*, 1394−1401.
17. Reinhart, G. D., Hartleip, S. B., and Symcox, M. M. (1989) *Proc. Natl. Acad. Sci. U.S.A. 86*, 4032−4036.
18. Symcox, M. M., and Reinhart, G. D. (1992) *Anal. Biochem. 206*, 394−399.
19. Frieden, C. (1964) *J. Biol. Chem. 239*, 3522−3531.
20. Cha, S. (1968) *J. Biol. Chem. 243*, 820−825.
21. Reinhart, G. D. (1985) *Biochemistry 24*, 7166−7172.
22. Tlapak-Simmons, V., and Reinhart, G. D. (1994) *Arch. Biochem. Biophys. 308*, 226−230.
23. Braxton, B. L., Mullins, L. S., Raushel, F. M., and Reinhart, G. D. (1996) *Biochemistry 35*, 11918−11924.
24. Reinhart, G. D. (1989) in *Fluorescence Biomolecules* (Jameson, D. M., and Reinhart, G. D., Eds.) pp 195−216, Plenum Publishing Corp., New York.
25. Tlapak-Simmons, V., and Reinhart, G. D. (1998) *Biophys. J. 75*, 1010−1015.
26. Wells, C. M., and Di Cera, E. (1992) *Biochemistry 31*, 11721−11730.
27. Braxton, B. L., Tlapak-Simmons, V. L., and Reinhart, G. D. (1994) *J. Biol. Chem. 269*, 47−50.
28. Uyeda, K., and Racker, E. (1965) *J. Biol. Chem. 240*, 4682−4688.
29. Antonini, E., Wyman, J., Rossi-Fanelli, A., Jr., and Caputo, A. (1962) *J. Biol. Chem. 237*, 2773−2777.
30. De Cristofaro, R., Fenton, J. W., and Di Cera, E. (1992) *Biochemistry 31*, 1147−1153.

BI001769R